

WEDGE: Web-Image Assisted Domain Generalization for Semantic Segmentation

Namyup Kim^{1*} Taeyoung Son¹ Cuiling Lan² Wenjun Zeng² Suha Kwak¹

¹ Department of Computer Science and Engineering, POSTECH, Korea

² Microsoft Research Asia, Beijing, China

Abstract

Domain generalization for semantic segmentation is highly demanded in real applications, where a trained model is expected to work well in previously unseen domains. One challenge lies in the lack of data which could cover the diverse distributions of the possible unseen domains for training. In this paper, we propose a WEB-image assisted Domain GENeralization (WEDGE) scheme, which is the first to exploit the diversity of web-crawled images for generalizable semantic segmentation. To explore and exploit the real-world data distributions, we collect a web-crawled dataset which presents large diversity in terms of weather conditions, sites, lighting, camera styles, etc. We also present a method which injects the style representation of the web-crawled data into the source domain on-the-fly during training, which enables the network to experience images of diverse styles with reliable labels for effective training. Moreover, we use the web-crawled dataset with predicted pseudo labels for training to further enhance the capability of the network. Extensive experiments demonstrate that our method clearly outperforms existing domain generalization techniques.

1 Introduction

Semantic segmentation has played crucial roles in many applications like autonomous vehicle and augmented reality. Recent advances in this field are mainly attributed to the development of deep neural networks, whose success depends heavily on the availability of a large-scale annotated dataset for training. However, creating large training datasets is prohibitively expensive since it demands manual annotation of pixel-level class labels. To mitigate this problem, synthetic image datasets have been introduced (Richter et al. 2016; Ros et al. 2016). They provide a large amount of labeled images for training at minimal cost of construction. Also, they can simulate scenes that are rarely observed in the real world yet must be considered in training (e.g., accidents in autonomous driving scenarios).

When learning semantic segmentation using synthetic images, it is essential to close the gap between the synthetic and real domains caused by their appearance differences so as to avoid performance degradation of learned models on real-world images. Most of existing solutions to this issue

*This work was done when Namyup Kim was an intern at Microsoft Research Asia.

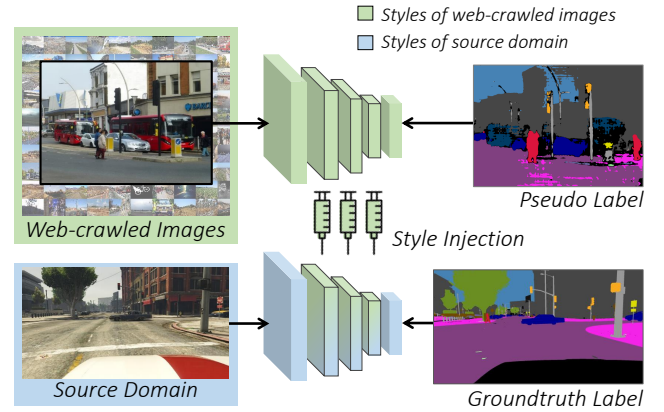


Figure 1: A conceptual illustration of WEDGE. It utilizes web-crawled images for domain generalization in two different ways. First, it replaces neural styles of synthetic training images with those of unlabeled web images, which give illusions of diverse real images while learning using labeled synthetic images. To this end, we introduce *style injection*, a non-parametric and on-the-fly style adjustment method. Second, the web images are used for supervised learning with their predicted pseudo labels to further enhance generalization capability.

belong to the category of domain adaptation, which aims at adapting models trained on synthetic images (i.e., source domain) to real-world images (i.e., target domain). In general, domain adaptation methods assume a single, particular target domain and train models using images from both of labeled source and unlabeled target domains (Hoffman et al. 2016; Tsai et al. 2018, 2019; Vu et al. 2019; Zou et al. 2018; Li, Yuan, and Vasconcelos 2019; Zou et al. 2019; Pan et al. 2020; Kang et al. 2020). Unfortunately, this setting limits applicability of learned models since, when deployed, models can face multiple and diverse target domains (e.g., geolocations and weather conditions in the case of autonomous vehicle) that are latent at the training stage.

As a more realistic solution to the problem, we study *domain generalization* for semantic segmentation. The goal of this task is to learn models that generalize well to various target domains without having access to images of the target domains in training. A pioneer work (Yue et al. 2019)

achieves the generalization by forcing segmentation models to be invariant to random style variations of input image. However, this method is costly since it applies an image-to-image translator (Zhu et al. 2017) to every source image several times for the style randomization. Further, random styles are given by a small number of images sampled from ImageNet (Deng et al. 2009), thus often irrelevant to target applications and hard to cover a wide range of real-world image styles. Meanwhile, follow-up research (Chen et al. 2020) encourages the representations learned using synthetic images to be similar with those of an ImageNet pretrained network. This method is unfortunately also limited by the knowledge of ImageNet.

In this paper, we propose a WEB-image assisted Domain Generalization scheme, dubbed *WEDGE*, which overcomes the limitations of previous work by using real and application-relevant images crawled from web repositories (e.g., Flickr). The crawling process demands no or minimal human intervention as it only asks search keywords that are determined directly by target application (e.g., “driving + road” for autonomous driving) or classes appearing in the source domain images. Moreover, unlike those of ImageNet, the retrieved images can be used for self-supervised learning as well as for stylization since they are expected to be relevant to target application.

As illustrated in Fig. 1, *WEDGE* utilizes images crawled from the Web in two different ways. First, it replaces neural styles of synthetic training images with those of web-crawled images on-the-fly during training. This helps enhance the generalization by giving illusions of diverse real images while exploiting groundtruth labels of synthetic images. For this purpose, we introduce a *style injection* module that conducts the style manipulation in a feature level at low cost. As it is substantially more efficient than the image-to-image translator used in Yue et al. (2019), it allows to perform the stylization on-the-fly using a large number of web images as style references in training.

Second, the web-crawled images are used as additional training data with pseudo segmentation labels. To this end, the entire training procedure is divided into two stages. In the first stage, a segmentation model is trained with the style injection module, and the web-crawled images are used only for stylization. The learned model is then applied to the web-crawled images to estimate their pseudo labels. The second stage is identical to the former, except that it also utilizes the web-crawled images as training data by taking their pseudo labels as supervision.

To demonstrate the efficacy of *WEDGE*, we adopt each of the GTA5 (Richter et al. 2016) and SYNTHIA (Ros et al. 2016) datasets as the source domain for training, and evaluate trained models on three different real image datasets (Cordts et al. 2016; Yu et al. 2020; Neuhold et al. 2017). Experimental results demonstrate that *WEDGE* enables segmentation models to generalize well to multiple unseen real domains and clearly outperforms existing methods. In summary, the contribution of this paper is three-fold:

- To the best of our knowledge, *WEDGE* is the first that attempts to utilize web-crawled images for domain generalizable semantic segmentation. These images facilitate

self training based on the realistic data which may better approximate unseen testing domains.

- We introduce a style injection module, which helps achieve the generalization by giving illusions of reality while having reliable labels inherited from source domain images. This allows us to utilize a large number of real image styles on-the-fly during training.
- *WEDGE* outperforms existing domain generalization techniques (Yue et al. 2019; Chen et al. 2020; Choi et al. 2021) in every experiment.

2 Related Work

Domain Adaptive Semantic Segmentation

With the advent of synthetic datasets (Richter et al. 2016; Ros et al. 2016), unsupervised domain adaptation has been widely studied for semantic segmentation. This task is allowed to use both of labeled synthetic and unlabeled real data for training. Most of existing solutions to the task are divided into two categories: (1) *Distribution alignment* (Hoffman et al. 2016; Zhang, David, and Gong 2017; Tsai et al. 2018, 2019; Vu et al. 2019), and (2) *Self-training* (Zou et al. 2018; Li, Yuan, and Vasconcelos 2019; Zou et al. 2019; Pan et al. 2020). The former aims at aligning distributions of synthetic and real data in a common feature space. To this end, Hoffman et al. (2016) propose feature-level domain-adversarial learning. Based on this, follow-up studies have been proposed to align the distributions in the image level (Hoffman et al. 2018) and in the prediction space (Tsai et al. 2018, 2019; Vu et al. 2019). On the other hand, self-training methods exploit unlabeled data for supervised learning through their pseudo labels. In particular, they focus on improving the quality of pseudo labels by learning semantic segmentation and image translation bidirectionally (Li, Yuan, and Vasconcelos 2019), alleviating class imbalance issues in pseudo labels (Zou et al. 2018, 2019), and learning texture invariant representation using randomly stylized source data (Kim and Byun 2020).

However, applications of these methods are limited since they assume a single target domain. In contrast, our work aims at generalizing well to multiple latent target domains without having access to target domain data.

Domain Generalizable Semantic Segmentation

The goal of domain generalization is to learn models that well generalize to previously unseen domains (Muandet, Balduzzi, and Schölkopf 2013; Gan, Yang, and Gong 2016). Early approaches address this task mostly for classification (Li et al. 2018b, 2017, 2018a; Pan et al. 2018), but recent research demonstrates its potential for semantic segmentation (Pan et al. 2018; Yue et al. 2019; Chen et al. 2020). For example, Pan et al. (2018) tackle this problem by a feature normalization operation designed for learning domain invariant features, while Chen et al. (2020) encourage the representation learned on a source domain to be similar with that of an ImageNet pretrained model. Meanwhile, Yue et al. (2019) propose to learn features invariant to random style variations of input, and establish an evaluation protocol for domain generalizable semantic segmentation.

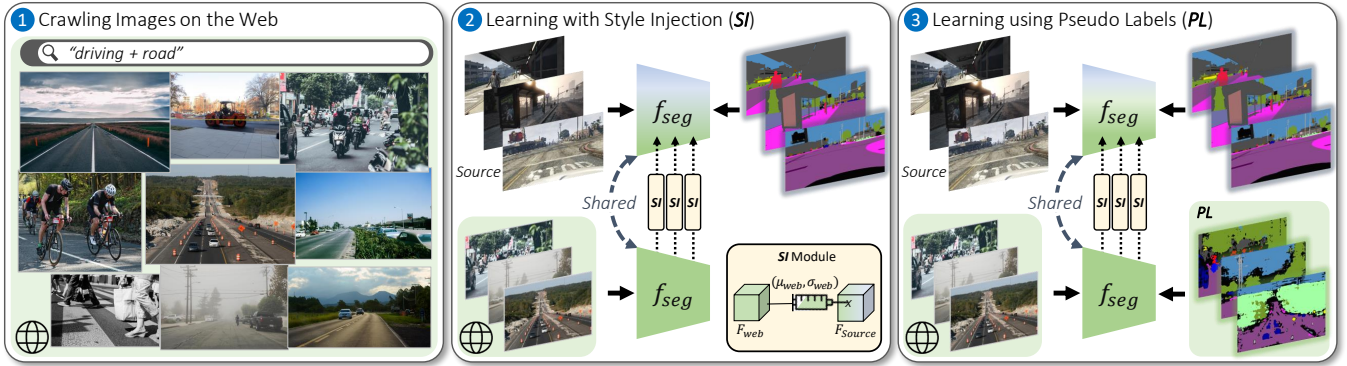


Figure 2: Overall framework of WEDGE. (1) Crawling real and task-relevant images from the Web automatically. (2) Learning semantic segmentation while transferring feature statistics of web images to features of synthetic training images in the source domain. (3) Further training the model using both source images and web-crawled images with predicted pseudo labels.

The main difference of ours from the previous work is that ours explores and exploits real images on the Web which enable models to experience a variety of real domains during training with no human intervention.

Learning Using Data on the Web

Modern recognition models tend to be data-hungry, yet the amount of training data is usually limited. Data on the Web have been exploited to alleviate this issue. Early studies utilize web-crawled images and videos for learning concept recognition by using their search keywords as pseudo labels (Chen, Shrivastava, and Gupta 2013; Divvala, Farhadi, and Guestrin 2014; Chen and Gupta 2015), and for object localization via clustering images (Chen, Shrivastava, and Gupta 2013; Divvala, Farhadi, and Guestrin 2014) or by motion segmentation (Prest et al. 2012). Motivated by recent advances in pseudo labeling, a large-scale web data have been used for supervised learning with their pseudo labels, which is known as webly supervised learning. For image classification, Niu, Veeraraghavan, and Sabharwal (2018) present a reliable way to utilize search keywords as pseudo class labels. For semantic segmentation, Hong et al. (2017) and Lee et al. (2019) compute pseudo labels by segmenting web videos using attentions drawn by an image classifier. Motivated by these methods, we present the first that makes use of web-crawled images for domain generalization.

Neural Style Transfer

It has been known that the style of an image can be represented by statistics of neural network features. A pioneer work by Gatys, Ecker, and Bethge (2016) shows that an image style can be captured by the Gram matrix (*i.e.*, channel-wise correlations) of a feature map and transferred by matching the matrices. Johnson, Alahi, and Fei-Fei (2016) further enhance this technique to transfer a neural style to arbitrary content images. Recent approaches suggest more elaborate style transfer techniques. Huang and Belongie (2017) demonstrate that the channel-wise mean and standard deviation of a feature map represent image style effectively. Also, Nam and Kim (2018) and Kim et al. (2020) propose to use different normalization operations that are complementary

to each other in selective manners.

Style injection in WEDGE is motivated by these techniques, in particular Huang and Belongie (2017). However, style injection is different in that it aims to perform feature stylization, rather than image stylization.

3 Proposed Method

WEDGE is divided into three steps as follows. Overall training flow is illustrated in Fig. 2.

1. *Crawling images from web repositories automatically.*
2. *The first stage of training with style injection (SI):* Learning a segmentation model on the source dataset while injecting styles of the web-crawled images to its intermediate features for training.
3. *The second stage of training using pseudo labels (PI):* Further training the model using the web-crawled images and their pseudo segmentation labels as well as the source dataset.

Details of each step are presented in the remainder of this section.

Crawling Images from the Web

We collect 4,904 images by crawling on Flickr, through the search keyword “driving + road” to find images relevant to the target application scenario, *i.e.*, autonomous driving. Examples of the collected images are presented in Fig. 3.

Using these images for domain generalization has several advantages. First of all, they offer a large variety of real image styles as illustrated in Fig. 3, which *potentially cover testing domains*. This is vital for achieving generalization to unseen domains. Second, they are not random but mostly relevant to target applications due to the use of search keywords, which enables us to use them for supervised learning given their pseudo labels. Last, they are accessible with minimal human intervention since the crawling process above is fully automated given a query.

The web-crawled images are often different from those of the source domain in terms of semantic layout, and could partly contain irrelevant contents due to the ambiguity of search keyword and errors from search engine. WEDGE is robust against these issues for the following reasons. In

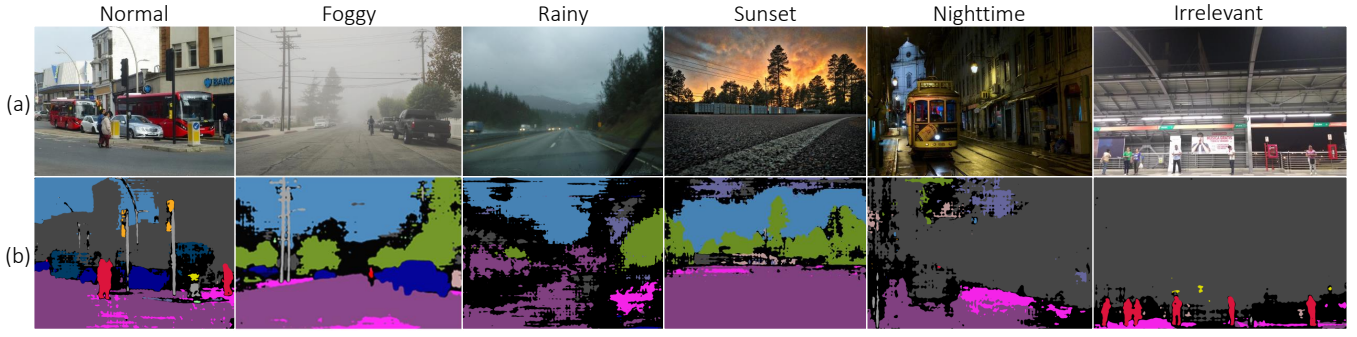


Figure 3: Qualitative examples of web images and their pseudo labels generated by the segmentation model with Resnet101 backbone trained by the first stage of WEDGE. (a) Input images. (b) Pseudo segmentation labels. These images demonstrate large diversity of the web images, which is vital for achieving generalization to multiple latent test domains.

the first stage of training, the style injection module exploits only styles of the web images while disregarding their contents. In the second stage, irrelevant parts of an image tend to be ignored in pseudo segmentation labels due to their unreliable class predictions (*i.e.*, low confidence).

Stage 1: Learning with Style Injection (SI)

At each iteration of the training of the segmentation network, a source image I^s is coupled with a web-crawled image I^w that is randomly sampled. Style injection starts by computing neural styles of I^w . Following recent approaches to style transfer (Huang and Belongie 2017; Nam and Kim 2018; Park et al. 2020), we represent a neural style of I^w as statistics of its intermediate features from the segmentation network. Let $F^{w,l} \in \mathbb{R}^{H \times W \times C}$ be the feature map of I^w from the l^{th} convolution block of the network. A neural style of I^w is estimated by the channel-wise mean and standard deviation of $F^{w,l}$, $\mu(F^{w,l}) \in \mathbb{R}^C$ and $\sigma(F^{w,l}) \in \mathbb{R}^C$, which are computed by

$$\mu_c(F^{w,l}) = \frac{1}{HW} \sum_{i=1}^H \sum_{j=1}^W F_{ijc}^{w,l}, \quad (1)$$

$$\sigma_c(F^{w,l}) = \sqrt{\frac{1}{HW} \sum_{i=1}^H \sum_{j=1}^W (F_{ijc}^{w,l} - \mu_c(F^{w,l}))^2}. \quad (2)$$

The style injection module replaces the feature statistics of I^s with those of I^w while feed-forwarding I^s through the segmentation network; Fig. 4 illustrates this process. To be specific, the module applied to the feature map of I^s from the l^{th} convolution block, denoted by $F^{s,l}$, transforms the feature map as

$$\tilde{F}^{s,l} = \sigma(F^{w,l}) \frac{F^{s,l} - \mu(F^{s,l})}{\sigma(F^{s,l})} + \mu(F^{w,l}). \quad (3)$$

The above process of style injection is applied to multiple convolution blocks of the network, in particular lower blocks since features of deeper layers are known to be less sensitive to style variations; more details for implementation can be found in Sec. 4. Note that the style injection module is designed as non-parametric, which enables effective and low-cost feature adjustment.

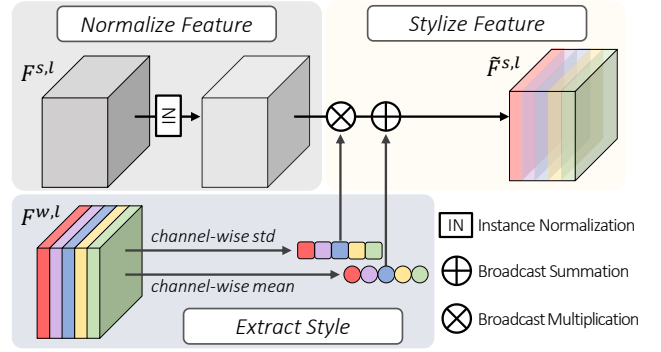


Figure 4: Details of the style injection. (1) Extracting style representations of a web image in the form of feature statistics. (2) Normalizing the source image features to discard their own styles. (3) Stylizing the normalized source features by the style representations of the web image.

Finally, the network is trained by the pixel-wise cross-entropy loss with the segmentation label of the source image I^s . Let P^s and Y^s denote the segmentation prediction and the groundtruth label of I^s , respectively. Then the loss is formulated as

$$\mathcal{L}_{\text{seg}}(P^s, Y^s) = -\frac{1}{N} \sum_{i=1}^H \sum_{j=1}^W \sum_{k=1}^C Y_{ijk}^s \log P_{ijk}^s, \quad (4)$$

where $N = H \times W$. Although this loss is applied only to the source domain, its gradients with respect to parameters will act as if the network takes real domain images as input thanks to the style injection. Note that, in this stage, I^w is used only as a style reference.

Stage 2: Learning Using Pseudo Labels (PL)

Once the first stage is completed, the learned model can be used to generate pseudo labels of the web images. The pseudo labels allow us to exploit the web images for supervised learning of the segmentation network, which further enhances the generalization capability of the model by learning it directly on a variety of real-world images.

Let $P^w \in \mathbb{R}^{H \times W \times C}$ be the segmentation prediction of the network given I^w as input. The pseudo segmentation label of I^w , denoted by $\tilde{Y}^w \in \{0, 1\}^{H \times W \times C}$, is obtained by

choosing pixels with highly reliable predictions and labeling them with the classes of maximum scores:

$$\tilde{Y}_{ijc}^w = \begin{cases} 1, & \text{if } c = \underset{k}{\operatorname{argmax}} P_{ijk}^w \text{ and } h(P_{ij}^w) < \tau \\ 0, & \text{otherwise} \end{cases}, \quad (5)$$

where $P_{ij}^w \in \mathbb{R}^C$ denotes the class probability distribution of the pixel (i, j) , $h(\cdot)$ indicates the entropy, and τ is a hyper-parameter. Note that we regard the prediction P_{ij}^w unreliable when its entropy is high, *i.e.*, $h(P_{ij}^w) \geq \tau$; in this case, the pixel is assigned no label and ignored during training. Examples of the pseudo labels are presented in Fig. 3.

The second stage of training utilizes both of the source and the web-crawled images for supervised learning of the network. It is basically the same with the first stage including the style injection, except that the segmentation loss is now applied to P^w as well as P^s . The total loss for the second stage is thus given by a linear combination of two segmentation losses:

$$\mathcal{L}(P^s, Y^s, P^w, \tilde{Y}^w) = \mathcal{L}_{\text{seg}}(P^s, Y^s) + \mathcal{L}_{\text{seg}}(P^w, \tilde{Y}^w), \quad (6)$$

where \mathcal{L}_{seg} is the pixel-wise cross-entropy loss as given in Eq. (4).

4 Experiments

In this section, we first present experimental settings in detail, then demonstrate the effectiveness of WEDGE through extensive results. Effectiveness of style injection, pseudo labeling, and other design choices of WEDGE are investigated by ablation studies.

Experimental Setting

Source datasets. As a synthetic source domain for training, we use either the GTA5 (Richter et al. 2016) or the SYNTHIA (Ros et al. 2016) datasets. GTA5 consists of 24,966 images and shares the same set of 19 semantic classes with the real test datasets. Note that we remove 36 images of smallest file sizes from the dataset since they are non-informative, *e.g.*, blacked-out images. Meanwhile, SYNTHIA contains 9,400 images, whose annotations cover only 16 classes of the real test datasets. Thus, we take only these 16 classes into account when evaluating models trained on SYNTHIA.

Test datasets. As unseen target domains for evaluation, we choose the validation splits of the Cityscapes (Cordts et al. 2016), BDD100k Segmentation (BDDS) (Yu et al. 2020) and Mapillary (Neuhof et al. 2017) datasets. The Cityscapes and BDDS datasets have 500 and 1,000 validation images, respectively, and they are labeled for the same 19 classes. 2,000 validation images of the Mapillary dataset are annotated for 66 classes. By following the protocol of He et al. (2020), we merge these classes to obtain the same 19 classes of the Cityscapes dataset.

Web-crawled images. From Flickr, we search for images whose widths are larger than or equal to 760 pixels, and with no copyright reserved (*i.e.*, CC0) for their public use in future work, using the search keyword “driving + road”. As a result, 4,904 web images in total are collected. Note that,

Methods	Backbone	G → C	G → B	G → M
IBN-Net	VGG16	-	-	-
	ResNet50	29.64	-	-
	ResNet101	-	-	-
ASG	VGG16	31.47	-	-
	ResNet50	31.89	-	-
	ResNet101	-	-	-
DRPC	VGG16	36.11	31.56	32.25
	ResNet50	37.42	32.14	34.12
	ResNet101	42.53	38.72	38.05
RobustNet	VGG16	-	-	-
	ResNet50	36.58	35.20	40.33
	ResNet101	-	-	-
WEDGE (Ours)	VGG16	38.55	37.49	43.80
	ResNet50	38.15	36.14	43.21
	ResNet101	43.60	41.62	48.82

Table 1: Quantitative results in mIoU of domain generalization from (G)TA5 to (C)ityscapes, (B)DDS, and (M)apillary.

Methods	Backbone	S → C	S → B	S → M
DRPC	VGG16	35.52	29.45	32.27
	ResNet50	35.65	31.53	32.74
	ResNet101	37.58	34.34	34.12
WEDGE (Ours)	VGG16	36.52	30.35	34.83
	ResNet50	38.33	31.18	38.65
	ResNet101	40.31	35.57	42.33

Table 2: Quantitative results in mIoU of domain generalization from (S)YNTHIA to (C)ityscapes, (B)DDS, and (M)apillary.

given these conditions, the crawling process was done automatically, and the retrieved images are used as-is without modification.

Networks and their training details. Following the current state of the art (Yue et al. 2019), we adopt DeepLabv2 (Chen et al. 2017) with various backbone networks, VGG16 (Simonyan and Zisserman 2015), ResNet50 (He et al. 2016), and ResNet101 (He et al. 2016), as our segmentation networks. They are first pretrained on ImageNet (Deng et al. 2009), then trained with the source dataset and our web-crawled images using SGD with momentum of 0.9 and weight decay of $5e-4$; the initial learning rate is $2e-4$ for the first stage (SI) and $1e-4$ for the second stage (PL). We set τ in Eq. (5) to $5e-2$ for all experiments.

Where to inject styles. Styles of web images are injected into the feature maps output by the 1st, 2nd, and 3rd residual blocks for ResNet101, and those of 2nd, 3rd, and 4th residual blocks for ResNet50. The slight change of injection points between the networks is to keep a certain percentage of layers affected by the style injection. For this reason, in the case of VGG16, we inject styles into the outputs of its 2nd and 3rd convolutional blocks as it is shallower than the ResNet architectures. The effects of injection points on performance are investigated in the supplementary material.

Comparisons with the State of the Art

WEDGE is compared with existing domain generalization techniques, IBN-Net (Pan et al. 2018), AGS (Chen et al. 2020), DRPC (Yue et al. 2019) and RobustNet (Choi et al.

	VGG16			ResNet50			ResNet101		
	<i>Src. only</i>	SI (Stage 1)	PL (Stage 2)	<i>Src. only</i>	SI (Stage 1)	PL (Stage 2)	<i>Src. only</i>	SI (Stage 1)	PL (Stage 2)
G \rightarrow C	29.28	35.89	38.55	28.29	33.61	38.15	34.28	41.88	43.60
G \rightarrow B	27.98	35.88	37.49	29.16	33.30	36.14	32.96	40.13	41.62
G \rightarrow M	35.68	42.44	43.80	40.46	41.12	43.21	41.31	47.26	48.82
G _{avg}	30.98	38.07	39.95	32.64	36.01	39.17	36.18	43.09	44.68
S \rightarrow C	26.79	34.40	36.52	27.06	36.08	38.33	29.96	38.14	40.31
S \rightarrow B	22.56	27.01	30.35	23.96	27.64	31.18	24.28	29.29	35.57
S \rightarrow M	30.60	32.33	34.83	31.67	37.67	38.65	36.19	40.32	42.33
S _{avg}	26.65	31.25	33.90	27.56	33.80	36.05	30.14	35.92	39.40

Table 3: Performance of WEDGE for domain generalization from (G)TA5 and (S)YNTHIA to (C)ityscapes, (B)DDS, and (M)apillary.

2021), using two source domains (GTA5, SYNTHIA), three test domains (Cityscapes, BDDS, Mapillary), and three different backbone networks (VGG16, ResNet50, ResNet101). As summarized in Table 1 and 2, WEDGE clearly outperforms all the previous arts in all the 18 experiments; its outstanding performance suggests the advantages of using web-crawled images for domain generalization.

In-depth Analysis on WEDGE

Detailed performance analysis. To investigate the contribution of each training stage in WEDGE, we measure its performance at each stage for all experiments we have conducted so far. The results are summarized in Table 3. As shown in the table, the first stage using style injection most contributes to the performance in most experiments, which demonstrates the effectiveness of using web-crawled images and our style injection module for domain generalization. This achievement is remarkable, especially when considering that web images could be erroneous or irrelevant to the test domains. Thanks to our style injection modules, WEDGE can exploit only diverse and realistic styles of web images while disregarding their contents that may be irrelevant. The second stage also leads to non-trivial performance improvement, particularly in the generalization from SYNTHIA to BDDS, which imply the semantics or layouts of pseudo labels on SYNTHIA is more similar to those of BDDS than the other datasets.

Qualitative results. Fig. 6 presents qualitative results of WEDGE and its baseline. The examples in the figure show that the first stage of WEDGE recovers most of the ill-classified pixels, and even finds out objects that are missing in the baseline results. Also, its second stage further improves the segmentation quality by correcting dotted errors and capturing fine details of object shapes.

Effect of the number of web-crawled images. We investigate the effect of the number of web-crawled images by evaluating performance of a segmentation model trained by WEDGE with different numbers of web-crawled images. In Fig. 5, these models are compared in terms of segmentation quality on the three target datasets. As shown in the figure, the generalization capability of the model can be substantially improved by using only 1,000 web images, while using the whole web dataset further improves performance. To be specific, when using 1,000 web images, the average mIoU

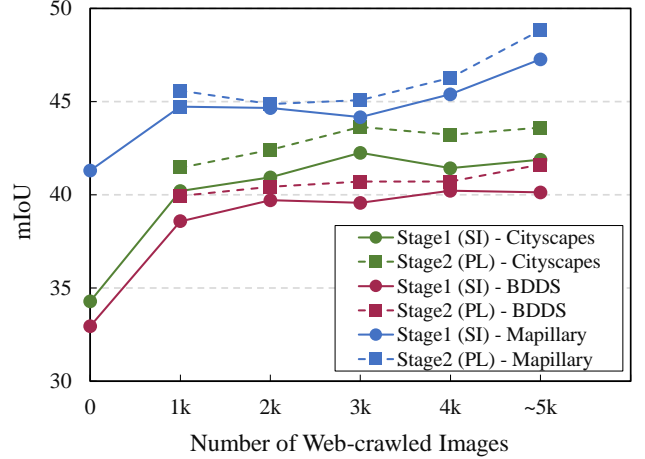


Figure 5: Domain generalization performance of WEDGE versus the number of web images. In all experiments ResNet101 is used as backbone.

Style reference	G \rightarrow C	G \rightarrow B	G \rightarrow M
None (source only)	34.28	32.96	41.31
ImageNet	41.73	38.88	45.75
Web images: “indoor”	42.01	40.86	47.65
Web images: “driving+road”	43.60	41.62	48.82

Table 4: Domain generalization performance of WEDGE with different types of style reference. In all experiments ResNet101 is used as backbone.

over the 3 test datasets is 42.3%, lacking only 2.4% compared to the average performance of our final model. The results also indicate that WEDGE consistently enhances the generalization performance when increasing the number of web-crawled images.

Effect of using task-relevant web images. The contribution of our crawling strategy is demonstrated by comparing WEDGE with its variants relying on other types of style references instead of the task-relevant web images. Specifically, we utilize images sampled from the ImageNet dataset and web images crawled by the search keyword “indoor”, both of which are irrelevant to the target task. Also, the number of style references is set to 5,000 for fair comparisons to WEDGE. Note that since these images are totally irrelevant to the target task, they are not suitable for pseudo labeling thus are used only for style injection. As shown in



Figure 6: Qualitative results of WEDGE and its baseline using ResNet101 backbone and trained on the GTA5 dataset.

Methods	$G \rightarrow C$	$G \rightarrow B$	$G \rightarrow M$
Source only	34.28	32.96	41.31
AdaptOutput _w	32.06	35.17	41.64
WEDGE-Stage 1	41.88	40.13	47.26

Table 5: Comparison to a variant of AdaptOutput (Tsai et al. 2018) that is adapted to web-crawled images instead of test domains, in the domain generalization setting using GTA5. In all experiments ResNet101 is used as backbone.

Table 4, our method using task-relevant web images (*i.e.*, “driving+road”) clearly outperforms the others. Using the real yet irrelevant images improves performance, suggesting the robustness of our method, but the results are still inferior to those of our method, meaning that our crawling strategy is useful and using relevant images matters.

Style injection vs. domain-adversarial learning. To further understand the advantages of the style injection, we compare WEDGE with AdaptOutput (Tsai et al. 2018) in the web-image assisted domain generalization setting. Specifically, AdaptOutput is trained using the same source data and adapted to the web images by domain-adversarial learning; this variant of AdaptOutput is denoted by AdaptOutput_w. Since AdaptOutput_w does not exploit pseudo labels of web images, it is compared to the first stage of WEDGE using only style injection for a fair comparison. As shown in Table 5, AdaptOutput_w improves performance marginally or

even degrades performance, while the first stage of WEDGE consistently and substantially enhances the segmentation quality. These results suggest that the domain adversarial learning is not an effective method for utilizing web images in the context of domain generalization. Aligning the source and web images cannot efficiently extend the scope of feature spaces to cover unseen testing domains. In contrast, increasing the diversity of training images (feature styles) increases the generalization capability.

5 Conclusion

We propose WEDGE, the first web-image assisted domain generalization scheme for learning semantic segmentation. It explores and exploits web images that depict large diversity of real world scenes, which potentially cover latent test domains thus help improve generalization capability of trained models. We propose effective ways to utilize the web-crawled images, namely style injection and pseudo labeling, which lead to consistent and substantial performance improvement over its baseline on test domains. WEDGE clearly outperformed existing domain generalization techniques in all experiments, and is even as competitive as domain adaptation methods using test domain data that are not accessible in domain generalization. Extensive ablation studies also demonstrated that WEDGE is able to utilize noisy and irrelevant web-crawled images reliably and is not sensitive to their number in training.

References

- Chen, L.-C.; Papandreou, G.; Kokkinos, I.; Murphy, K.; and Yuille, A. L. 2017. DeepLab: Semantic Image Segmentation with Deep Convolutional Nets, Atrous Convolution, and Fully Connected CRFs. *IEEE Transactions on Pattern Analysis and Machine Intelligence (TPAMI)*.
- Chen, W.; Yu, Z.; Wang, Z.; and Anandkumar, A. 2020. Automated synthetic-to-real generalization. In *Proc. International Conference on Machine Learning (ICML)*.
- Chen, X.; and Gupta, A. 2015. Webly supervised learning of convolutional networks. In *Proc. IEEE International Conference on Computer Vision (ICCV)*.
- Chen, X.; Shrivastava, A.; and Gupta, A. 2013. Neil: Extracting visual knowledge from web data. In *Proc. IEEE International Conference on Computer Vision (ICCV)*.
- Choi, S.; Jung, S.; Yun, H.; Kim, J. T.; Kim, S.; and Choo, J. 2021. RobustNet: Improving Domain Generalization in Urban-Scene Segmentation via Instance Selective Whitening. In *Proc. IEEE Conference on Computer Vision and Pattern Recognition (CVPR)*.
- Cordts, M.; Omran, M.; Ramos, S.; Rehfeld, T.; Enzweiler, M.; Benenson, R.; Franke, U.; Roth, S.; and Schiele, B. 2016. The Cityscapes Dataset for Semantic Urban Scene Understanding. In *Proc. IEEE Conference on Computer Vision and Pattern Recognition (CVPR)*.
- Deng, J.; Dong, W.; Socher, R.; Li, L.-J.; Li, K.; and Fei-Fei, L. 2009. ImageNet: A large-scale hierarchical image database. In *Proc. IEEE Conference on Computer Vision and Pattern Recognition (CVPR)*.
- Divvala, S. K.; Farhadi, A.; and Guestrin, C. 2014. Learning everything about anything: Webly-supervised visual concept learning. In *Proc. IEEE Conference on Computer Vision and Pattern Recognition (CVPR)*.
- Gan, C.; Yang, T.; and Gong, B. 2016. Learning attributes equals multi-source domain generalization. In *Proc. IEEE Conference on Computer Vision and Pattern Recognition (CVPR)*.
- Gatys, L. A.; Ecker, A. S.; and Bethge, M. 2016. Image style transfer using convolutional neural networks. In *Proceedings of the IEEE conference on computer vision and pattern recognition*, 2414–2423.
- He, K.; Zhang, X.; Ren, S.; and Sun, J. 2016. Deep Residual Learning for Image Recognition. In *Proc. IEEE Conference on Computer Vision and Pattern Recognition (CVPR)*.
- He, Y.; Rahimian, S.; Schiele, B.; and Fritz, M. 2020. Segmentations-Leak: Membership Inference Attacks and Defenses in Semantic Image Segmentation. In *European Conference on Computer Vision*, 519–535. Springer.
- Hoffman, J.; Tzeng, E.; Park, T.; Zhu, J.-Y.; Isola, P.; Saenko, K.; Efros, A.; and Darrell, T. 2018. Cycada: Cycle-consistent adversarial domain adaptation. In *Proc. International Conference on Machine Learning (ICML)*.
- Hoffman, J.; Wang, D.; Yu, F.; and Darrell, T. 2016. Fcns in the wild: Pixel-level adversarial and constraint-based adaptation. *arXiv preprint arXiv:1612.02649*.
- Hong, S.; Yeo, D.; Kwak, S.; Lee, H.; and Han, B. 2017. Weakly Supervised Semantic Segmentation Using Web-Crawled Videos. In *Proc. IEEE Conference on Computer Vision and Pattern Recognition (CVPR)*, 2224–2232.
- Huang, X.; and Belongie, S. 2017. Arbitrary style transfer in real-time with adaptive instance normalization. In *Proc. IEEE International Conference on Computer Vision (ICCV)*.
- Johnson, J.; Alahi, A.; and Fei-Fei, L. 2016. Perceptual losses for real-time style transfer and super-resolution. In *European conference on computer vision*, 694–711. Springer.
- Kang, G.; Wei, Y.; Yang, Y.; Zhuang, Y.; and Hauptmann, A. 2020. Pixel-Level Cycle Association: A New Perspective for Domain Adaptive Semantic Segmentation. In *Proc. Neural Information Processing Systems (NeurIPS)*.
- Kim, J.; Kim, M.; Kang, H.; and Lee, K. H. 2020. U-GAT-IT: Unsupervised Generative Attentional Networks with Adaptive Layer-Instance Normalization for Image-to-Image Translation. In *Proc. International Conference on Learning Representations (ICLR)*.
- Kim, M.; and Byun, H. 2020. Learning texture invariant representation for domain adaptation of semantic segmentation. In *Proceedings of the IEEE/CVF Conference on Computer Vision and Pattern Recognition*, 12975–12984.
- Lee, J.; Kim, E.; Lee, S.; Lee, J.; and Yoon, S. 2019. Frame-to-frame aggregation of active regions in web videos for weakly supervised semantic segmentation. In *Proc. IEEE International Conference on Computer Vision (ICCV)*.
- Li, D.; Yang, Y.; Song, Y.-Z.; and Hospedales, T. 2018a. Learning to generalize: Meta-learning for domain generalization. In *Proc. AAAI Conference on Artificial Intelligence (AAAI)*.
- Li, D.; Yang, Y.; Song, Y.-Z.; and Hospedales, T. M. 2017. Deeper, broader and artier domain generalization. In *Proc. IEEE International Conference on Computer Vision (ICCV)*.
- Li, H.; Pan, S. J.; Wang, S.; and Kot, A. C. 2018b. Domain generalization with adversarial feature learning. In *Proc. IEEE Conference on Computer Vision and Pattern Recognition (CVPR)*.
- Li, Y.; Yuan, L.; and Vasconcelos, N. 2019. Bidirectional learning for domain adaptation of semantic segmentation. In *Proc. IEEE Conference on Computer Vision and Pattern Recognition (CVPR)*.
- Luo, Y.; Zheng, L.; Guan, T.; Yu, J.; and Yang, Y. 2019. Taking a closer look at domain shift: Category-level adversaries for semantics consistent domain adaptation. In *Proc. IEEE Conference on Computer Vision and Pattern Recognition (CVPR)*.
- Muandet, K.; Balduzzi, D.; and Schölkopf, B. 2013. Domain generalization via invariant feature representation. In *Proc. International Conference on Machine Learning (ICML)*.
- Nam, H.; and Kim, H.-E. 2018. Batch-Instance Normalization for Adaptively Style-Invariant Neural Networks. In *Proc. Neural Information Processing Systems (NeurIPS)*.

- Neuhold, G.; Ollmann, T.; Rota Bulò, S.; and Kotschieder, P. 2017. The mapillary vistas dataset for semantic understanding of street scenes. In *Proc. IEEE International Conference on Computer Vision (ICCV)*.
- Niu, L.; Veeraraghavan, A.; and Sabharwal, A. 2018. Webly supervised learning meets zero-shot learning: A hybrid approach for fine-grained classification. In *Proc. IEEE Conference on Computer Vision and Pattern Recognition (CVPR)*.
- Pan, F.; Shin, I.; Rameau, F.; Lee, S.; and Kweon, I. S. 2020. Unsupervised intra-domain adaptation for semantic segmentation through self-supervision. In *Proc. IEEE Conference on Computer Vision and Pattern Recognition (CVPR)*.
- Pan, X.; Luo, P.; Shi, J.; and Tang, X. 2018. Two at once: Enhancing learning and generalization capacities via ibn-net. In *Proc. European Conference on Computer Vision (ECCV)*.
- Park, T.; Zhu, J.-Y.; Wang, O.; Lu, J.; Shechtman, E.; Efros, A. A.; and Zhang, R. 2020. Swapping Autoencoder for Deep Image Manipulation. In *Proc. Neural Information Processing Systems (NeurIPS)*.
- Prest, A.; Leistner, C.; Civera, J.; Schmid, C.; and Ferrari, V. 2012. Learning object class detectors from weakly annotated video. In *Proc. IEEE Conference on Computer Vision and Pattern Recognition (CVPR)*.
- Richter, S. R.; Vineet, V.; Roth, S.; and Koltun, V. 2016. Playing for data: Ground truth from computer games. In *Proc. European Conference on Computer Vision (ECCV)*.
- Ros, G.; Sellart, L.; Materzynska, J.; Vazquez, D.; and Lopez, A. M. 2016. The synthia dataset: A large collection of synthetic images for semantic segmentation of urban scenes. In *Proc. IEEE Conference on Computer Vision and Pattern Recognition (CVPR)*.
- Simonyan, K.; and Zisserman, A. 2015. Very deep convolutional networks for large-scale image recognition. In *Proc. International Conference on Learning Representations (ICLR)*.
- Tsai, Y.-H.; Hung, W.-C.; Schuster, S.; Sohn, K.; Yang, M.-H.; and Chandraker, M. 2018. Learning to adapt structured output space for semantic segmentation. In *Proc. IEEE Conference on Computer Vision and Pattern Recognition (CVPR)*.
- Tsai, Y.-H.; Sohn, K.; Schuster, S.; and Chandraker, M. 2019. Domain adaptation for structured output via discriminative patch representations. In *Proc. IEEE International Conference on Computer Vision (ICCV)*.
- Vu, T.-H.; Jain, H.; Bucher, M.; Cord, M.; and Pérez, P. 2019. Advent: Adversarial entropy minimization for domain adaptation in semantic segmentation. In *Proc. IEEE Conference on Computer Vision and Pattern Recognition (CVPR)*.
- Yu, F.; Chen, H.; Wang, X.; Xian, W.; Chen, Y.; Liu, F.; Madhavan, V.; and Darrell, T. 2020. Bdd100k: A diverse driving dataset for heterogeneous multitask learning. In *Proc. IEEE Conference on Computer Vision and Pattern Recognition (CVPR)*.
- Yue, X.; Zhang, Y.; Zhao, S.; Sangiovanni-Vincentelli, A.; Keutzer, K.; and Gong, B. 2019. Domain randomization and pyramid consistency: Simulation-to-real generalization without accessing target domain data. In *Proc. IEEE International Conference on Computer Vision (ICCV)*.
- Zhang, Y.; David, P.; and Gong, B. 2017. Curriculum domain adaptation for semantic segmentation of urban scenes. In *Proc. IEEE International Conference on Computer Vision (ICCV)*.
- Zhu, J.-Y.; Park, T.; Isola, P.; and Efros, A. A. 2017. Unpaired image-to-image translation using cycle-consistent adversarial networks. In *Proceedings of the IEEE international conference on computer vision*, 2223–2232.
- Zou, Y.; Yu, Z.; Kumar, B.; and Wang, J. 2018. Unsupervised domain adaptation for semantic segmentation via class-balanced self-training. In *Proc. European Conference on Computer Vision (ECCV)*.
- Zou, Y.; Yu, Z.; Liu, X.; Kumar, B.; and Wang, J. 2019. Confidence regularized self-training. In *Proc. IEEE International Conference on Computer Vision (ICCV)*.

Appendix

Advantages of Feature-level Style Injection

Since WEDGE injects style representations in feature levels, one may wonder its advantages over image-level style transfer. This section demonstrates the effectiveness of WEDGE, especially its style injection (SI) module, compared to image-level style transfer. To this end, we adopt AdaIN (Huang and Belongie 2017), exploiting feature statistics as style representation like WEDGE. We generate 100,000 stylized GTA5 (Richter et al. 2016) images by AdaIN using web-crawled images as style references; a few examples are shown in Fig. 7. We then train a segmentation model on the stylized GTA5 dataset.

As summarized in Table 6, we compare the model of the 1st stage of WEDGE (SI only) with the model trained on the stylized GTA5 images generated by AdaIN. The results show WEDGE using SI outperforms AdaIN on all experimental settings except G→B with ResNet50 (He et al. 2016). Moreover, our feature-level approach has another benefit over the image-level counterpart in terms of efficiency. AdaIN requires an additional network for style transfer. On the other hand, SI in WEDGE is non-parametric and adjusting feature statistics of source images by those of web-crawled images, thus demands a much lower computational cost than AdaIN.

Sensitivity to Hyper-parameter τ

This section demonstrates the impact of the thresholding parameter τ on the quality of pseudo labels in terms of semantic segmentation performance. Specifically, pseudo segmentation labels are generated by using τ , which is a hyper-parameter that filters out unreliable predictions. To this end, we design multiple variants of our model that are trained from different pseudo segmentation labels generated from various τ . The pseudo segmentation label of I^w , denoted by $\tilde{Y}^w \in \{0, 1\}^{H \times W \times C}$, is obtained by choosing pixels with highly reliable predictions and labeling them with the classes of maximum scores:

$$\tilde{Y}_{ijc}^w = \begin{cases} 1, & \text{if } c = \underset{k}{\operatorname{argmax}} P_{ijk}^w \text{ and } h(P_{ij}^w) < \tau \\ 0, & \text{otherwise} \end{cases}, \quad (7)$$

where $h(\cdot)$ indicates the entropy, $P_{ij}^w \in \mathbb{R}^C$ denotes the class probability distribution of the pixel (i, j) , and τ is a hyper-parameter. We sample τ from $\{0.1, 0.05, 0.01, 0.005\}$, where $\tau = 0.05$ means our model in the main paper.

As summarized in Fig. 8, the results are marginally different across the variation of the hyper-parameters, but the setting we adopt in the paper is slightly better than the others. Examples of the pseudo labels of web-crawled images

Methods	Backbone	Params	G → C	G → B	G → M
Deeplab-v2 (2017) +AdaIN	VGG16	53.1M	35.33	34.49	40.17
	ResNet50	48.6M	33.31	34.02	38.55
	ResNet101	67.6M	39.41	36.20	41.50
WEDGE (SI)	VGG16	29.6M	35.89	35.88	42.44
	ResNet50	25.1M	33.61	33.30	41.12
	ResNet101	44.0M	41.88	40.13	47.26

Table 6: Quantitative results in mIoU and parameters of domain generalization from (G)TA5 (Richter et al. 2016) to (C)ityscapes (Cordts et al. 2016), (B)DDS (Yu et al. 2020) and (M)appillary (Neuhof et al. 2017).

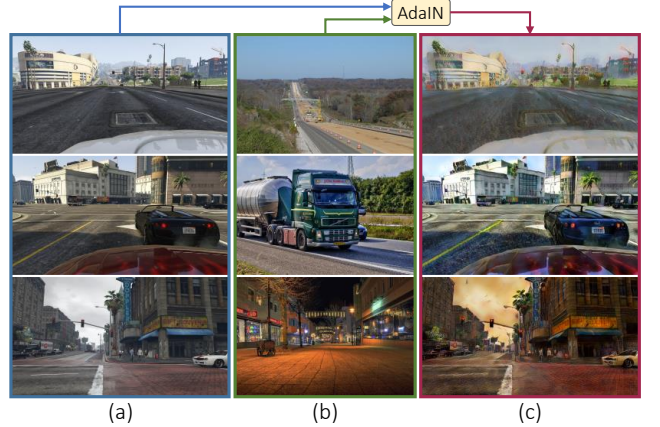


Figure 7: Examples of GTA5 images stylized by AdaIN. (a) Content images. (b) Style images. (c) Stylized images.

are presented in Fig. 9, which demonstrates both pros and cons of different threshold values. With a moderate thresholding (e.g., 0.1), the pseudo labels cover more real texture or parts of an object but have more noisy semantic labels. With a strict thresholding, on the other hand, the pseudo labels have more accurate semantic information but cover smaller regions of web-crawled images. The thresholding hyper-parameter we choose is in the middle, and leads to the best performance.

Details of Style Injection

Style representations of web-crawled images are injected into the feature maps output by 1th, 2nd, and 3rd residual blocks for ResNet101 (He et al. 2016), those of 2nd, 3rd, and 4th residual blocks for ResNet50 (He et al. 2016), and those of 2nd and 3rd blocks for VGG16 (Simonyan and Zisserman 2015). To verify the effectiveness of our method, this section presents ablation studies with various combinations of injection points. We present experimental results with ResNet101

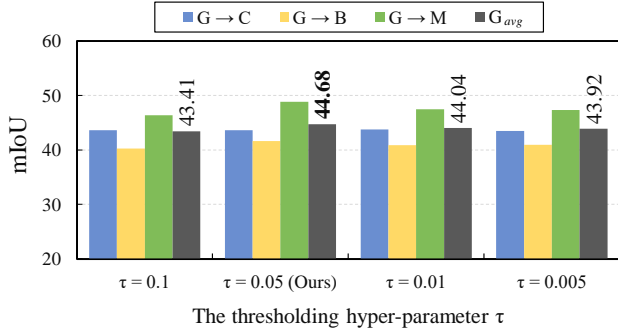


Figure 8: Performance of our ResNet101 backbone model trained with different thresholded pseudo labels from (G)TA5 (Richter et al. 2016) to (C)ityscapes (Cordts et al. 2016), (B)DDS (Yu et al. 2020) and (M)appillary (Neuhof et al. 2017). G_{avg} is the average performance of the three test domains. The performances across the set of hyper-parameters τ are marginally different.

combined with four different combinations in Table 7. The results show that semantic segmentation performance is degraded when 4th residual block is included. We suspect this is because deeper features are known to contain semantic information rather than styles, which makes them inappropriate for style injection. The comparison between the combination of {1st, 2nd} and {2nd, 3rd} residual blocks also shows relatively shallower layers are more proper for style injection than deeper ones. As a result, using the output feature maps from the {1st, 2nd, 3rd} residual blocks turn out to be the most effective combination for ResNet101. Therefore, we choose our injection points based on these observations when applying style injection to other backbone networks. We denote feature map outputs prior to the injection points are *affected*, as the distributions of features are transformed by the style injection. In ResNet101 backbone, the ratio of blocks affected by the injection, denoted by R_{inject}^{101} , is calculated by

$$R_{inject}^{101} = \frac{1 + 9 + 12 + 69}{101} = 90.1\%. \quad (8)$$

To maintain the similar ratio on ResNet50, we select {2nd, 3rd, 4th} blocks for the style injection, then the ratio of affected blocks in ResNet50 is

$$R_{inject}^{50} = \frac{1 + 9 + 12 + 18 + 9}{50} = 98\%. \quad (9)$$

If we use the injection points same as ResNet101 for ResNet50, the ratio can be only 80%. Therefore, we inject the style on {2nd, 3rd, 4th} blocks of ResNet50 by following the similar ratio of ResNet101 setting.

Table 8 shows experimental results with VGG16 combined with four different combinations of injection points. Since the network architecture of VGG16 is totally different and shallower compared to ResNet, the injection points are slightly changed. The results show that the combination of {2nd, 3rd} blocks performs the best than the other variants. The combinations including 2nd and 3rd blocks are better than the others. Moreover, the performance is degraded

Backbone	Injection points	mIoU		
		G \rightarrow C	G \rightarrow B	G \rightarrow M
ResNet101	{1, 2}	41.58	40.26	46.47
	{2, 3}	41.12	38.30	44.47
	{2, 3, 4}	39.10	35.50	43.94
	{1, 2, 3}	41.88	40.13	47.26

Table 7: Performance of the models with ResNet101 backbone on the setting from (G)TA5 to (C)ityscapes, (B)DDS and (M)appillary.

Backbone	Injection points	mIoU		
		G \rightarrow C	G \rightarrow B	G \rightarrow M
VGG16	{2, 3, 4}	34.50	34.05	39.92
	{3, 4}	30.82	29.65	36.61
	{2, 4}	32.87	33.40	38.41
	{2, 3}	35.89	35.88	42.44

Table 8: Performance of the models with VGG16 backbone on the setting from (G)TA5 to (C)ityscapes, (B)DDS and (M)appillary.

with the injection on the 4th block. The ratio of affected blocks from the injection is 43.8% which is a lower ratio than ResNet backbone. We assume the reason stems from the different architecture. To be specific, ResNet consists of multiple residual blocks with identity mapping, which are proven to be effective in maintaining low-level features.

Examples of Web-crawled Images

This section exhibits a part of our web-crawled dataset. Qualitative examples of the web-crawled images are presented in Fig. 12, which demonstrates the diversity of the images in terms of time, geolocation, weather condition, and so on. Such diversity enables WEDGE to achieve the generalization to latent real domains. Note that these images often depict entities and semantic layouts that are irrelevant to those of source (and target) domains. However, they are used as-is with no manual filtering process since the style injection and pseudo labeling of WEDGE offer reliable and effective ways to utilize them.

More Qualitative Results

We present qualitative examples of semantic segmentation results by WEDGE for both of Stage 1 (SI) and Stage 2 (SI+PL) in Fig. 10 and Fig. 11. In these figures, the semantic segmentation results are color-coded by following the standard Cityscapes color map (Cordts et al. 2016); the colors associated to the classes are exhibited in Table 9.

road	sidewalk	building	wall
fence	pole	traffic light	traffic sign
vegetation	terrain	sky	person
rider	car	truck	bus
train	motorbike	bicycle	

Table 9: The color code of classes on the test datasets.

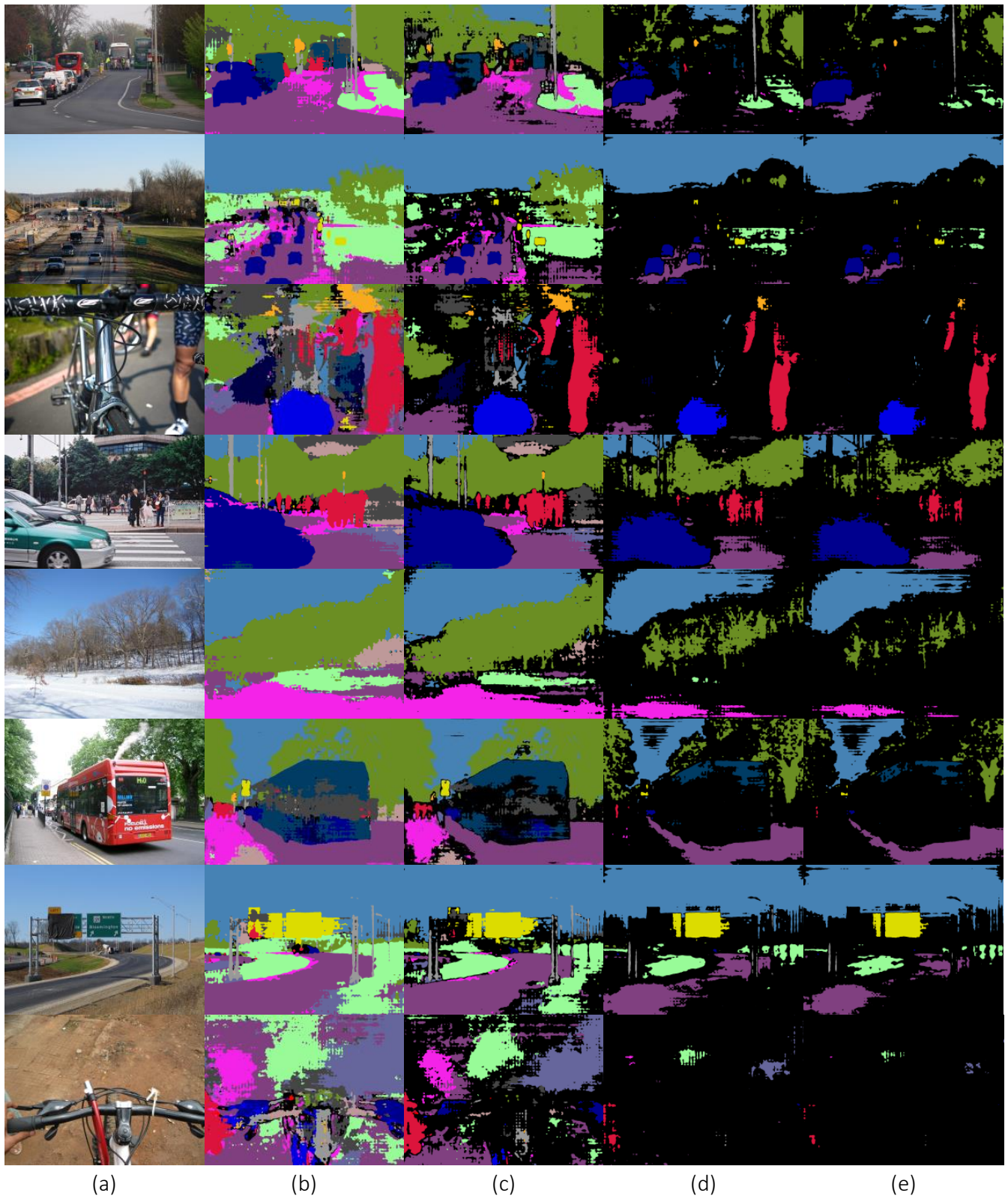


Figure 9: Examples of the pseudo labels with the different thresholding hyper-parameter τ . (a) Input images. Pseudo labels with (b) $\tau = 0.1$. (c) $\tau = 0.05$ (Ours). (d) $\tau = 0.01$. (e) $\tau = 0.005$.

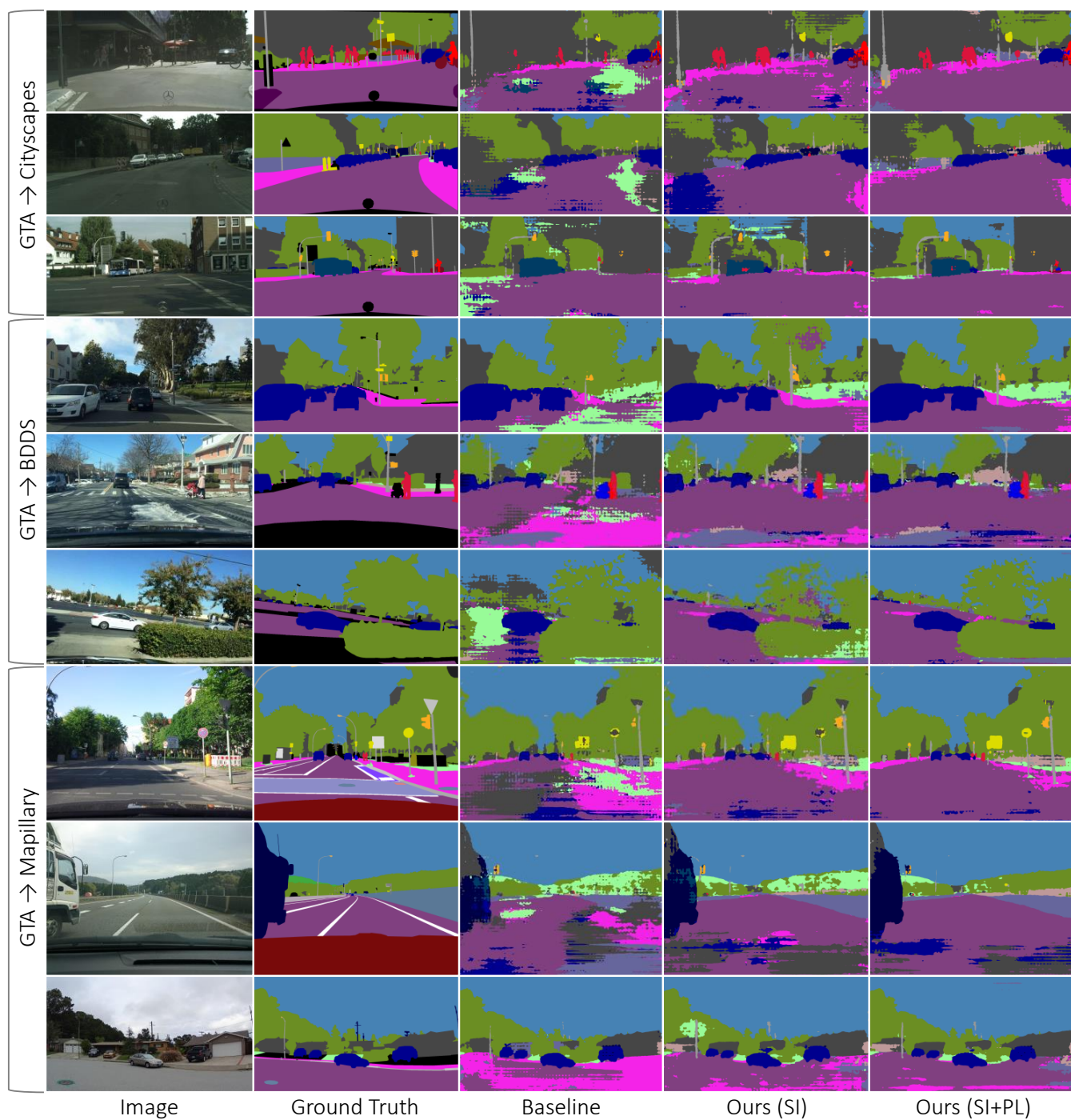


Figure 10: Qualitative results of WEDGE and its baseline using ResNet101 backbone and trained on the GTA5 dataset.

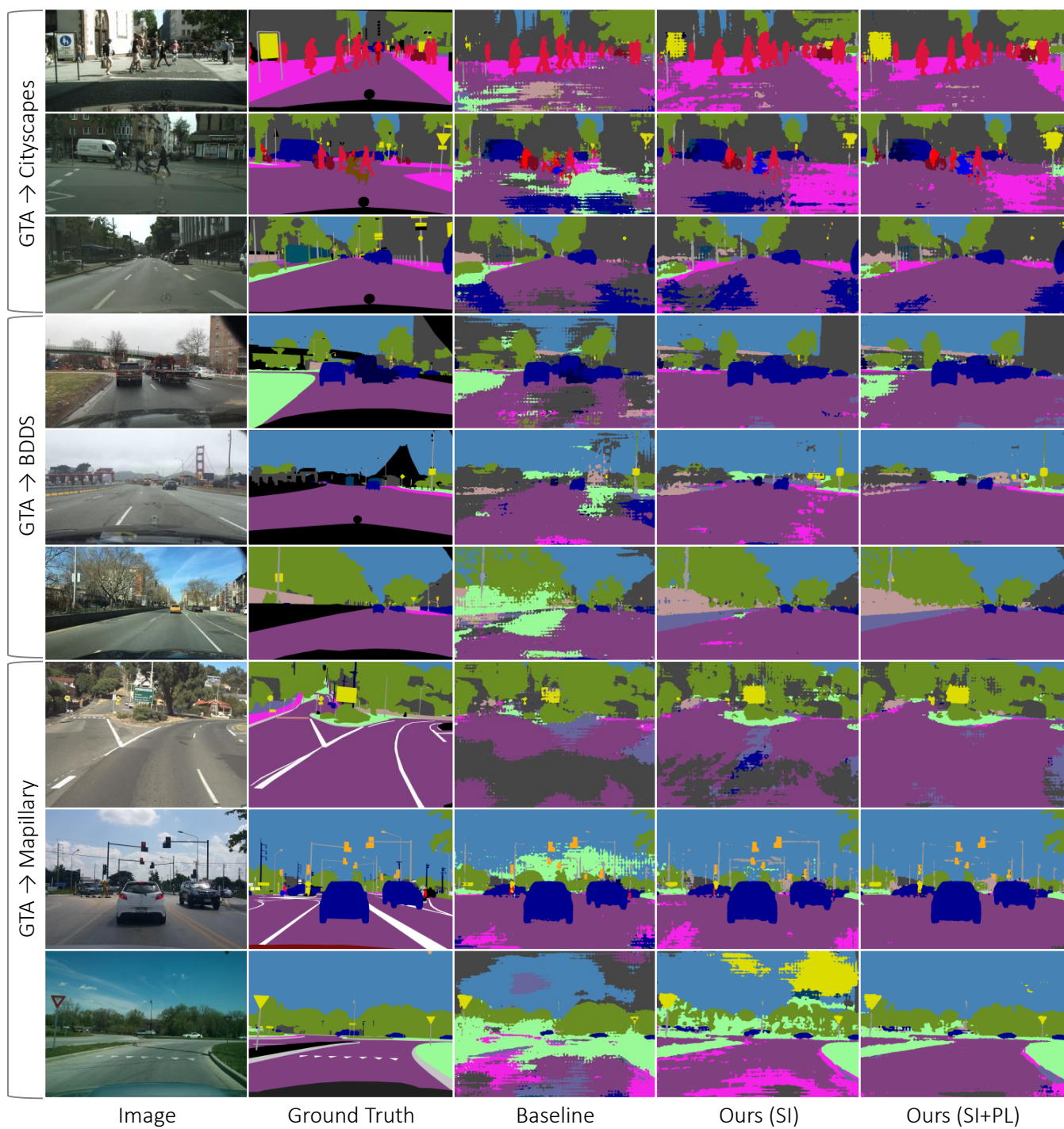


Figure 11: Qualitative results of WEDGE and its baseline using ResNet101 backbone and trained on the GTA5 dataset.



Figure 12: 500 random samples of the web-crawled images used in WEDGE.

Backbone	Method	$\text{Train w/ } T_{gt}$	road	sidew.	build.	wall	fence	pole	t-light	t-sign	vege.	terrain	sky	person	rider	car	truck	bus	train	motor.	bike	mIoU
VGG16	Baseline		76.0	15.6	68.0	13.0	17.3	16.9	21.0	6.9	75.4	14.6	65.9	44.8	6.7	73.5	16.3	8.0	0.1	16.1	0.5	29.3
	AdaptOutput (2018)	✓	87.3	29.8	78.6	21.1	18.2	22.5	21.5	11.0	79.7	29.6	71.3	46.8	6.5	80.1	23.0	26.9	0.0	10.6	0.3	35.0
	CLAN (2019)	✓	88.0	30.6	79.2	23.4	20.5	26.1	23.0	14.8	81.6	34.5	72.0	45.8	7.9	80.5	26.6	29.9	0.0	10.7	0.0	36.6
	ADVENT (2019)	✓	86.9	28.7	78.7	28.5	25.2	17.1	20.3	10.9	80.0	26.4	70.2	47.1	8.4	81.5	26.0	17.2	18.9	11.7	1.6	36.1
	PatchOutput (2019)	✓	87.3	35.7	79.5	32.0	14.5	21.5	24.8	13.7	80.4	32.0	70.5	50.5	16.9	81.0	20.8	28.1	4.1	15.5	4.1	37.5
	BDL (2019)	✓	89.2	40.9	81.2	29.1	19.2	14.2	29.0	19.6	83.7	35.9	80.7	54.7	23.3	82.7	25.8	28.0	2.3	25.7	19.9	41.3
	LTIR (2020)	✓	92.5	54.5	83.9	34.5	25.5	31.0	30.4	18.0	84.1	39.6	83.9	53.6	19.3	81.7	21.1	13.6	17.7	12.3	6.5	42.3
	DRPC (2019)	✗	84.6	31.5	76.3	25.4	17.2	28.2	21.5	13.7	80.7	26.8	74.9	47.5	15.8	77.1	22.2	22.7	1.7	8.9	9.7	36.1
	WEDGE (Ours)	✗	87.2	40.2	82.3	29.3	22.9	25.0	21.9	10.4	82.1	33.1	83.7	51.2	12.6	82.0	28.7	23.4	1.3	12.4	2.8	38.6
ResNet101	Baseline		70.3	15.8	67.8	12.2	13.2	18.8	28.7	14.2	80.1	10.5	67.4	51.6	24.9	52.6	35.4	30.4	0.6	22.7	34.1	34.3
	AdaptOutput (2018)	✓	86.5	36.0	79.9	23.4	23.3	23.9	35.2	14.8	83.4	33.3	75.6	58.5	27.6	73.7	32.5	35.4	3.9	30.1	28.1	42.4
	CLAN (2019)	✓	87.0	27.1	79.6	27.3	23.3	28.3	35.5	24.2	83.6	27.4	74.2	58.6	28.0	76.2	33.1	36.7	6.7	31.9	31.4	43.2
	ADVENT (2019)	✓	89.4	33.1	81.0	26.6	26.8	27.2	33.5	24.7	83.9	36.7	78.8	58.7	30.5	84.8	38.5	44.5	1.7	31.6	32.4	45.5
	PatchOutput (2019)	✓	92.3	51.9	82.1	29.2	25.1	24.5	33.8	33.0	82.4	32.8	82.2	58.6	27.2	84.3	33.4	46.3	2.2	29.5	32.3	46.5
	BDL (2019)	✓	91.0	44.7	84.2	34.6	27.6	30.2	36.0	36.0	85.0	43.6	83.0	58.6	31.6	83.3	35.3	49.7	3.3	28.8	35.6	48.5
	CRST (2019)	✓	91.0	55.4	80.0	33.7	21.4	37.3	32.9	24.5	85.0	34.1	80.8	57.7	24.6	84.1	27.8	30.1	26.9	26.0	42.3	47.1
	LTIR (2020)	✓	92.9	55.0	85.3	34.2	31.1	34.9	40.7	34.0	85.2	40.1	87.1	61.0	31.1	82.5	32.3	42.9	0.3	36.4	46.1	50.2
	PLCA (2020)	✓	84.0	30.4	82.4	35.3	24.8	32.2	36.8	24.5	85.5	37.2	78.6	66.9	32.8	85.5	40.4	48.0	8.8	29.8	41.8	47.7
	DRPC (2019)	✗	-	-	-	-	-	-	-	-	-	-	-	-	-	-	-	-	-	-	-	42.5
	WEDGE (Ours)	✗	86.1	17.3	81.7	26.3	24.2	29.5	29.9	34.5	81.8	25.6	81.8	59.2	24.8	82.2	37.9	37.7	3.5	23.9	40.6	43.6

Table 10: Performance in the generalization and adaptation from GTA5 to Cityscapes setting.

Backbone	Method	$\text{Train w/ } T_{gt}$	road	sidew.	build.	wall	fence	pole	t-light	t-sign	vege.	sky	person	rider	car	bus	motor.	bike	mIoU ₁₃	mIoU
VGG16	Baseline		14.6	16.8	58.8	4.7	0.2	25.2	2.45	11.8	64.9	75.9	51.6	14.0	54.4	17.8	2.5	13.21	30.7	26.8
	AdaptOutput (2018)	✓	78.9	29.2	75.5	-	-	-	0.1	4.8	72.6	76.7	43.4	8.8	71.1	16.0	3.6	8.4	37.6	-
	CLAN (2019)	✓	80.4	30.7	74.7	-	-	-	1.4	8.0	77.1	79.0	46.5	8.9	73.8	18.2	2.2	9.9	39.3	-
	ADVENT (2019)	✓	67.9	29.4	71.9	6.3	0.3	19.9	0.6	2.6	74.9	74.9	35.4	9.6	67.8	21.4	4.1	15.5	36.6	31.4
	PatchOutput (2019)	✓	72.6	29.5	77.2	3.5	0.4	21.0	1.4	7.9	73.3	79.0	45.7	14.5	69.4	19.6	7.4	16.5	39.6	33.7
	BDL (2019)	✓	72.0	30.3	74.5	-	-	-	10.2	25.2	80.5	80.0	54.7	23.2	72.7	24.0	7.5	44.9	46.1	-
	LTIR (2020)	✓	89.8	48.6	78.9	-	-	-	0.0	4.7	80.6	81.7	36.2	13.0	74.4	22.5	6.5	32.8	43.8	-
	DRPC (2019)	✗	77.5	30.7	78.6	5.6	0.2	26.7	10.6	16.1	75.2	76.5	44.1	15.8	69.9	14.7	8.6	17.6	41.2	35.5
	WEDGE (Ours)	✗	78.7	35.1	78.0	2.5	0.7	25.5	3.0	16.0	78.2	77.2	50.9	15.2	64.7	18.8	10.4	29.5	42.7	36.5
ResNet101	Baseline		30.1	14.0	69.7	7.44	0.1	22.7	7.7	11.7	73.9	82.1	54.6	17.6	48.5	13.5	7.73	18.0	34.5	30.0
	AdaptOutput (2018)	✓	79.2	37.2	78.8	10.5	0.3	25.1	9.9	10.5	78.2	80.5	53.5	19.6	67.0	29.5	21.6	31.3	45.9	39.5
	CLAN (2019)	✓	81.3	37.0	80.1	-	-	-	16.1	13.7	78.2	81.5	53.4	21.2	73.0	32.9	22.6	30.7	47.8	-
	ADVENT (2019)	✓	85.6	42.2	79.7	8.7	0.4	25.9	5.4	8.1	80.4	84.1	57.9	23.8	73.3	36.4	14.2	33.0	48.0	41.2
	PatchOutput (2019)	✓	82.4	38.0	78.6	8.7	0.6	26.0	3.9	11.1	75.5	84.6	53.5	21.6	71.4	32.6	19.3	31.7	46.5	40.0
	BDL (2019)	✓	86.0	46.7	80.3	-	-	-	14.1	11.6	79.2	81.3	54.1	27.9	73.7	42.2	25.7	45.3	51.4	-
	CRST (2019)	✓	67.7	32.2	73.9	10.7	1.6	37.4	22.2	31.2	80.8	80.5	60.8	29.1	82.8	25.0	19.4	45.3	50.1	43.8
	LTIR (2020)	✓	92.6	53.2	79.2	-	-	-	1.6	7.5	78.6	84.4	52.6	20.0	82.1	34.8	14.6	39.4	49.3	-
	PLCA (2020)	✓	82.6	29.0	81.0	11.2	0.2	33.6	24.9	18.3	82.8	82.3	62.1	26.5	85.6	48.9	26.8	52.2	54.0	46.8
	DRPC (2019)	✗	-	-	-	-	-	-	-	-	-	-	-	-	-	-	-	-	-	37.6
	WEDGE (Ours)	✗	72.3	25.9	77.6	19.66	0.4	26.8	16.1	21.7	73.5	82.2	58.7	24.9	76.6	32.18	16.8	19.7	46.0	40.3

Table 11: Performance in the generalization and adaptation from SYNTHIA to Cityscapes setting.

Comparison with Adaptation Methods

Since domain adaptation and generalization share similar objectives, we also compare WEDGE to the state-of-the-art domain adaptation techniques in the two adaptation settings, GTA5 to Cityscapes and SYNTHIA to Cityscapes. We provide the class-wise IoU of WEDGE with the previous domain adaptation and generalization in Table 10 and Table 11, for more detailed comparison. To unify the performance of domain adaptation and generalization methods, we report segmentation accuracies obtained by with VGG16 and ResNet101 backbones on the GTA5 (Richter et al. 2016) to Cityscapes (Cordts et al. 2016) and SYNTHIA (Ros et al. 2016) to Cityscapes settings. Because domain adaptation exploits test domain data, which are in contrast not accessible in domain generalization, direct comparisons between them are unfair. Nevertheless, WEDGE is as competitive as or even outperforms recently proposed domain adaptation techniques (Tsai et al. 2018; Luo et al. 2019; Vu et al. 2019; Tsai et al. 2019). Further, it achieves 91% and 86% of the best domain adaptation performance with VGG16 and ResNet101

backbones, respectively, in both of the GTA5 to Cityscapes and SYNTHIA to Cityscapes settings; *these results are impressive when considering that WEDGE does not have access to test domain images at all for training.*